

Electron–Phonon Interactions and Superconductivity in $(\text{Cu}_{0.5}\text{Tl}_{0.5})\text{Ba}_2\text{Ca}_3(\text{Cu}_{4-y}\text{Ti}_y)\text{O}_{12-\delta}$ ($y = 0, 0.25, 0.50, 0.75, 1.0$)

S. Qamar Abbas¹ · Nawazish A. Khan¹

Received: 20 August 2015 / Accepted: 26 September 2015 / Published online: 19 October 2015
© Springer Science+Business Media New York 2015

Abstract We have used two-step solid state reaction method for the synthesis of $(\text{Cu}_{0.5}\text{Tl}_{0.5})\text{Ba}_2\text{Ca}_3(\text{Cu}_{4-y}\text{Ti}_y)\text{O}_{12-\delta}$ ($y = 0, 0.25, 0.50, 0.75, 1.0$) superconductors at 880 °C. The oxygen contents in the samples were optimized by carrying out self-doping which is accomplished by post-annealed in flowing oxygen environment at 500 °C for approximately 5 h. The superconducting properties of all the samples were improved, after the self-doping of the carriers in the conducting planes. In the x-ray diffraction scans of the samples, the *a*-axis length of tetragonal unit cell increases whereas the *c*-axis decreases with increased Ti doping in the final compound. The Fourier transform infrared spectrometer (FTIR) absorption measurements of these samples have shown that the apical oxygen mode at 548 cm^{-1} and the planar oxygen mode at 596 cm^{-1} are softened with increased Ti doping. The origin of softening of planar oxygen mode lies in increase bond lengths of apical oxygen atoms promoted by larger covalent radius of Ti (1.32 Å) atoms relative to Cu (1.17 Å) atoms that in turn promotes the softening of the apical oxygen modes. Doped Ti (47.90 amu) atoms at the Cu (63.54 amu) sites initiate the an-harmonic oscillations resulting into the suppression of density of phonon modes. The suppression in the values of superconductivity parameters with Ti doping at the Cu sites shows the essential role of phonon in mechanism of high T_c superconductivity and hence the electron–phonons interactions. The

excess conductivity analyses (FIC) of conductivity data of oxygen-post-annealed samples have shown decrease in the mean field critical temperature, coherence length along the *c*-axis, interlayer coupling, and Fermi velocity with increase Ti doping. However, the values of B_c , B_{c1} , and $J_{c(0)}$ increase with Ti doping, showing increase in the population of the pinning centers.

Keywords Ti-doped superconductors · Oxygen post annealing · Phonon modes · Electron–phonon interactions · Excess conductivity analysis · Pinning centers

1 Introduction

The mysterious mechanism of high temperature superconductivity is still unknown, but there is clear consensus based on several experimental evidences that superconducting properties in oxide cuprates depend upon the optimum carrier concentration in the conducting CuO_2 planes [1–10]. The key structural unit in the oxide superconductors is a charge reservoir layer and the superconducting planes [i.e., $n\text{CuO}_2$ planes] where the superconductivity occurs. The carrier concentration can be controlled with the addition or removal of oxygen in the charge reservoir layer of the unit cell, which may be achieved by post-annealing the samples under appropriate conditions [11]. The density of oxygen in the charge reservoir layer can optimize the charge carrier's density in the conducting CuO_2 planes. The optimum density of mobile charge carriers in the conducting CuO_2 planes induces increase in Fermi wave vector K_F and Fermi velocity V_F of the carriers, which results in the improvement of superconducting properties of the final compound [12].

In this paper, we have presented the results of oxygen-post-annealed $(\text{Cu}_{0.5}\text{Tl}_{0.5})\text{Ba}_2\text{Ca}_3(\text{Cu}_{4-y}\text{Ti}_y)\text{O}_{12-\delta}$ ($y =$

✉ Nawazish A. Khan
nawazishalik2@yahoo.com;
nakhan@qau.edu.pk

¹ Materials Science Laboratory, Department of Physics, Quaid-i-Azam University, Islamabad 45320, Pakistan

0, 0.25, 0.50, 0.75, 1.0) superconductor samples. The substitution of Ti atom at copper site is carried out for understanding the role of phonon interaction in the mechanism of high temperature superconductivity [13–15]. Titanium atom has ground state electronic configuration $-3d^2.4s^2$ and atomic mass of Ti (47.9 amu) which is smaller than Cu (63.54 amu)

atoms. Due to this difference in masses, it is likely that doped Ti atoms may induce an-harmonic oscillations which will suppress the density of phonon in $\text{CuO}_2/\text{TiO}_2$ planes. Further, we had tried to find out the possible reasons behind the enhancement in superconducting parameters such as zero resistivity critical temperature $\{T_c(R = 0)\}$, cross-over

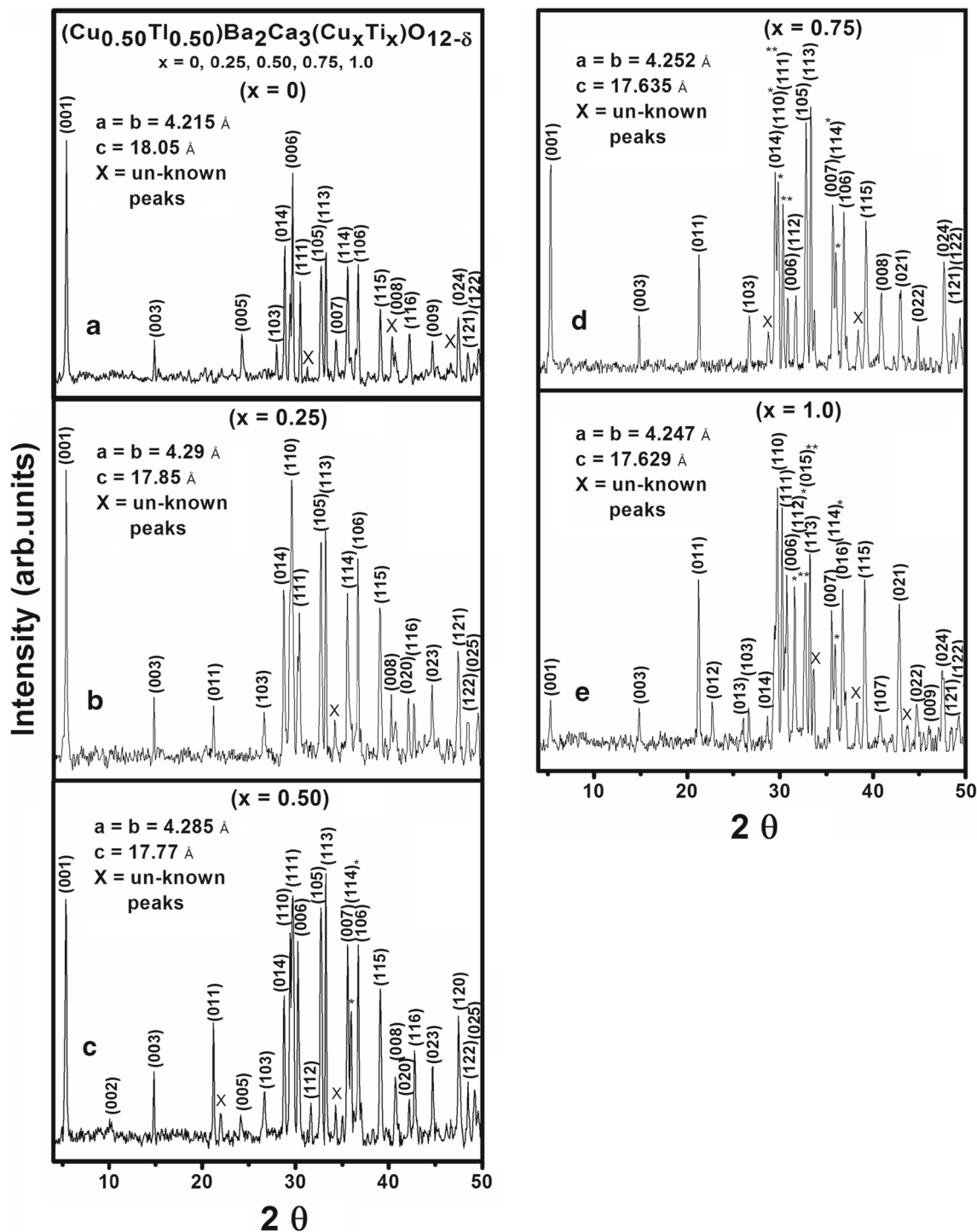


Fig. 1 a–c X-ray diffraction pattern of $(\text{Cu}_{0.5}\text{Tl}_{0.5})\text{Ba}_2\text{Ca}_3(\text{Cu}_{4-y}\text{Ti}_y)\text{O}_{12-\delta}$ ($y = 0, 0.25, 0.50$) as-prepared samples. d, e X-ray diffraction pattern of $(\text{Cu}_{0.5}\text{Tl}_{0.5})\text{Ba}_2\text{Ca}_3(\text{Cu}_{4-y}\text{Ti}_y)\text{O}_{12-\delta}$ ($y = 0.75, 1.0$) as-prepared samples

temperatures, zero-temperature coherence length $\{\xi_c(0)\}$, and interlayer coupling strength (J) from the fluctuation-induced conductivity (FIC) analysis. In high-temperature superconductors during the transport process well above T_c , the probability of the formation of Cooper pairs is always there and the causes of which is the thermal fluctuations.

2 Experimental

$(\text{Cu}_{0.5}\text{Tl}_{0.5})\text{Ba}_2\text{Ca}_3(\text{Cu}_{4-y}\text{Ti}_y)\text{O}_{12-\delta}$ ($y = 0, 0.25, 0.50, 0.75, 1.0$) samples were synthesized by two-step solid state reaction method. In the first stage $(\text{Cu}_{0.5})\text{Ba}_2\text{Ca}_3(\text{Cu}_{4-y}\text{Ti}_y)\text{O}_{12-\delta}$ ($y = 0, 0.25, 0.50, 0.75, 1.0$) precursor material was synthesized mixing weighted amounts of TiO_2 , $\text{Ba}(\text{NO}_3)_2$, $\text{Ca}(\text{NO}_3)_2 \cdot 4\text{H}_2\text{O}$, and $\text{Cu}(\text{CN})$ in a quartz mortar pestle followed by firing at 880°C in a quartz boat for 24 h. These samples were furnace cooled to room temperature and ground again for an hour and again fired at 880°C in an alumina boat for 24 h. These samples were furnace cooled to room temperature after each heat treatment. The precursor material was again ground for about an hour and mixed with Tl_2O_3 to give $(\text{Cu}_{0.5}\text{Tl}_{0.5})\text{Ba}_2\text{Ca}_3(\text{Cu}_{4-y}\text{Ti}_y)\text{O}_{12-\delta}$ ($y = 0, 0.25, 0.50, 0.75, 1.0$) as final reactants composition and pelletized under 3.8 tons/cm^2 . The pellets were then wrapped in a gold capsule and annealed for about 18 min at 880°C and then quenched to room temperature after the heat treatment. The samples were then post-annealed in the flowing oxygen environment at 500°C for approximately 5 h for the optimization of carrier density in the CuO_2 planes. The superconductivity characteristics of the oxygen-annealed samples were measured by resistivity, ac susceptibility, and Fourier transform infrared spectroscopic measurements. The Fourier transform infrared spectrometer (FTIR) absorption measurements were carried out by using Nicolet 5700 FTIR in the wave number range of

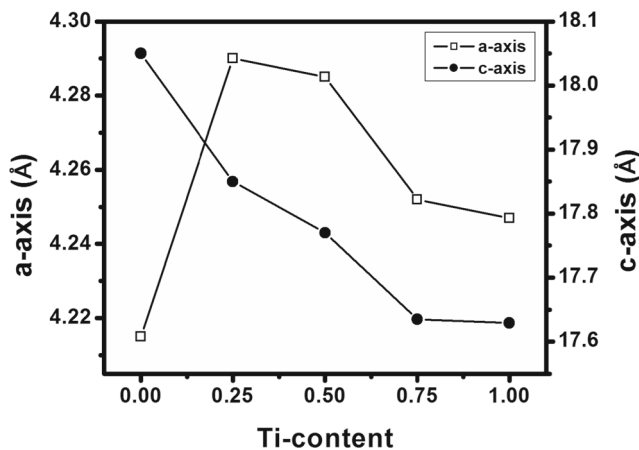


Fig. 2 Variation in c-axis and a-axis because of Ti content

$400\text{--}700 \text{ cm}^{-1}$. The crystal structure of the as-prepared samples was measured by x-ray diffraction scan using Bruker DX8 Focus employing $\text{CuK}\alpha$ radiations of wavelength 1.54056 \AA . The cell parameters were determined by check cell computer refinement program.

3 Theoretical Model for Analysis of Experimental Data

The fluctuation-induced conductivity (FIC) analysis is a state of the art theoretical analysis for the analysis of experimental data of cuprates superconductors that can play an essential role to unearth the intrinsic properties of the material well above the zero resistivity critical temperature $T_c(0)$, where the Cooper pair formation starts and imparts additional conductivity. There are two models that can give a very nice picture of superconducting fluctuations in inter-grains and intra-grains regions. AL model can be used for fluctuations both in inter-grains and intra-grains regions, while LD can be used only for fluctuations in intra-grains regions of layered superconductors [16, 17]. The excess conductivity is given by

$$\Delta\sigma(T) = \left[\frac{\rho_N(T) - \rho(T)}{\rho_N(T)\rho(T)} \right]$$

where $\rho(T)$ is the actually measured resistivity, and $\rho_N(T) = \alpha + \beta T$ is the normal-state resistivity of the samples extrapolated to resistivity at zero K; the α is an intercept, and β is a slope of a straight line. The total excess conductivity is generally comprised of two contributions, i.e.,

$$\Delta\sigma = \Delta\sigma_{\text{AL}} + \Delta\sigma_{\text{MT}}$$

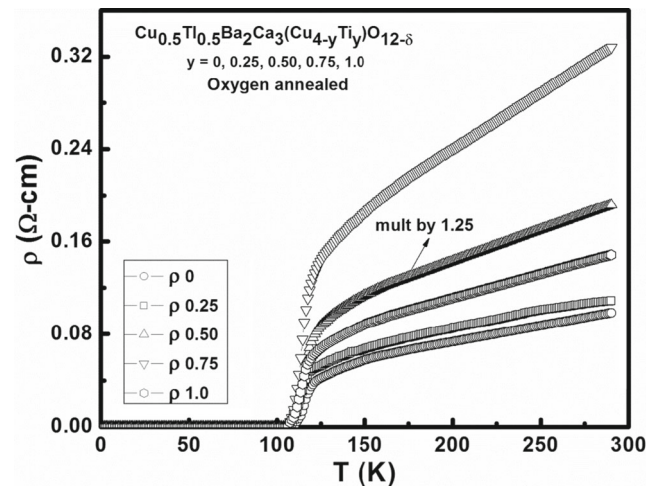


Fig. 3 Combined resistivity of oxygen-annealed $(\text{Cu}_{0.5}\text{Tl}_{0.5})\text{Ba}_2\text{Ca}_3(\text{Cu}_{4-y}\text{Ti}_y)\text{O}_{12-\delta}$ ($y = 0, 0.25, 0.50, 0.75, 1.0$) samples

The first term, according to AL model, is derived using microscopic approach by mean field theory and is considered as a direct contribution to para-conductivity [18]. The fluctuation-induced conductivity according to AL theory is given as

$$\Delta\sigma_{AL} = A\varepsilon^{-1}$$

where A is the fluctuation amplitude, λ is dimensional exponent, and ε is the reduce temperature

$$\varepsilon = \left[\frac{T - T_c^{mf}}{T_c^{mf}} \right]$$

T_c^{mf} is usually referred to as the mean field critical temperature, which separates the mean field region from the critical region [18, 19] and is determined from the point of inflection of the temperature derivative of resistivity ($d\rho/dT$). The exponent λ determines the dimensionality of the superconducting fluctuations and is given as $\lambda = 2 - D/2$; $\lambda = 3/2$, 1, and $1/2$ for one-, two-, and three-dimensional fluctuations, respectively. The fluctuation amplitude A for one-, two-, and three-dimensional fluctuations is given by [20]

$$A = \begin{cases} \frac{e^2}{32\hbar\xi_c(0)} & \text{for 3D fluctuation} \\ \frac{e^2}{16\hbar d} & \text{for 2D fluctuation} \\ \frac{e^2\xi_c(0)}{32\hbar s} & \text{for 1D fluctuation} \end{cases}$$

where e is the electron charge, $\xi_c(0)$ is the zero-temperature coherence length along c -axis, \hbar is the reduced Plancks constant, d is the effective layer thickness of the 2D system, and s is the cross-sectional area of the 1D system.

The physical microscopic parameters calculated from FIC analysis depend strongly on the dimensionality of the fluctuations. LD introduced the concept of interlayer coupling via Josephson coupling of adjacent layers close to the critical temperature. According to the LD model for

Fig. 4 Variation of $T_c(R = 0)$ and $T_c(\text{onset})$ of resistivity versus temperature graphs of both as-prepared and oxygen-annealed samples

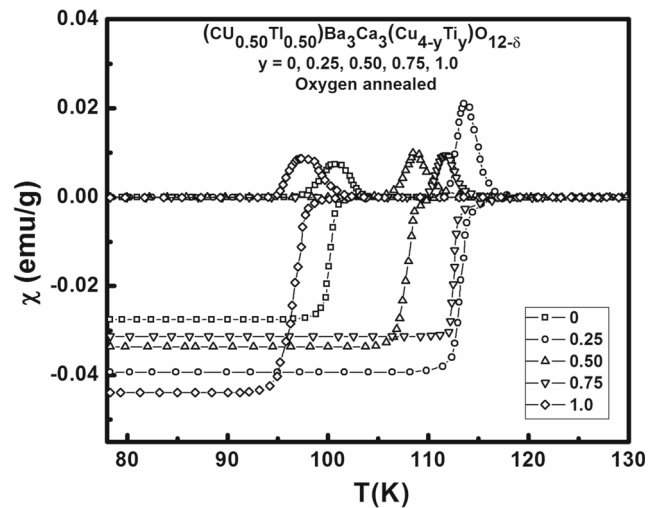
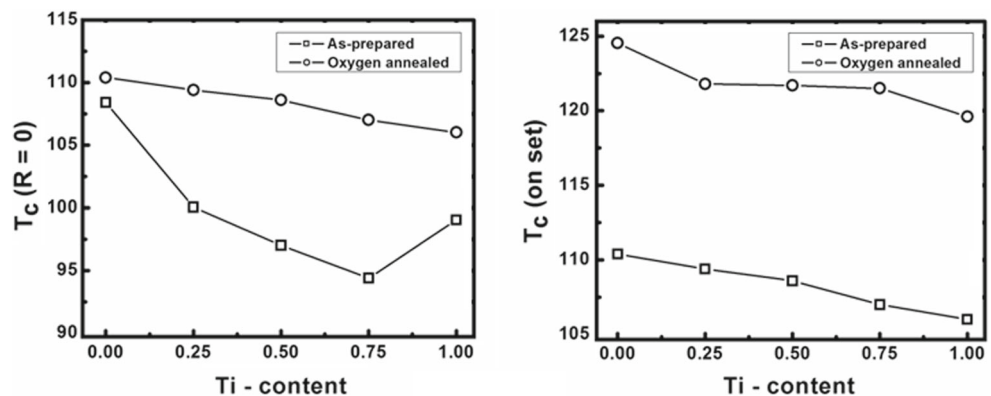


Fig. 5 The ac susceptibility versus temperature measurements of oxygen-annealed $(\text{Cu}_{0.5}\text{Tl}_{0.5})\text{Ba}_2\text{Ca}_3(\text{Cu}_{4-y}\text{Ti}_y)\text{O}_{12-\delta}$ ($y = 0, 0.25, 0.50, 0.75, 1.0$) samples

layered superconductors, the excess conductivity $\Delta\sigma_{LD}$ due to superconducting fluctuations is

$$\Delta\sigma_{LD} = \frac{e^2}{16\hbar d\varepsilon} (1 + 2\alpha)^{-\frac{1}{2}}$$

where α ,

$$\alpha = \frac{\alpha_0}{\varepsilon} = \left[\frac{\xi_c(0)}{d} \right]^2 2\varepsilon^{-1}$$

is a dimensionless coupling parameter. The cross-over from 2D to 3D is mainly found above the critical temperature known as cross-over temperature (T_0). The system has 3D fluctuations below this temperature and 2D fluctuations above this temperature, and the expression for T_0 according to the LD model is

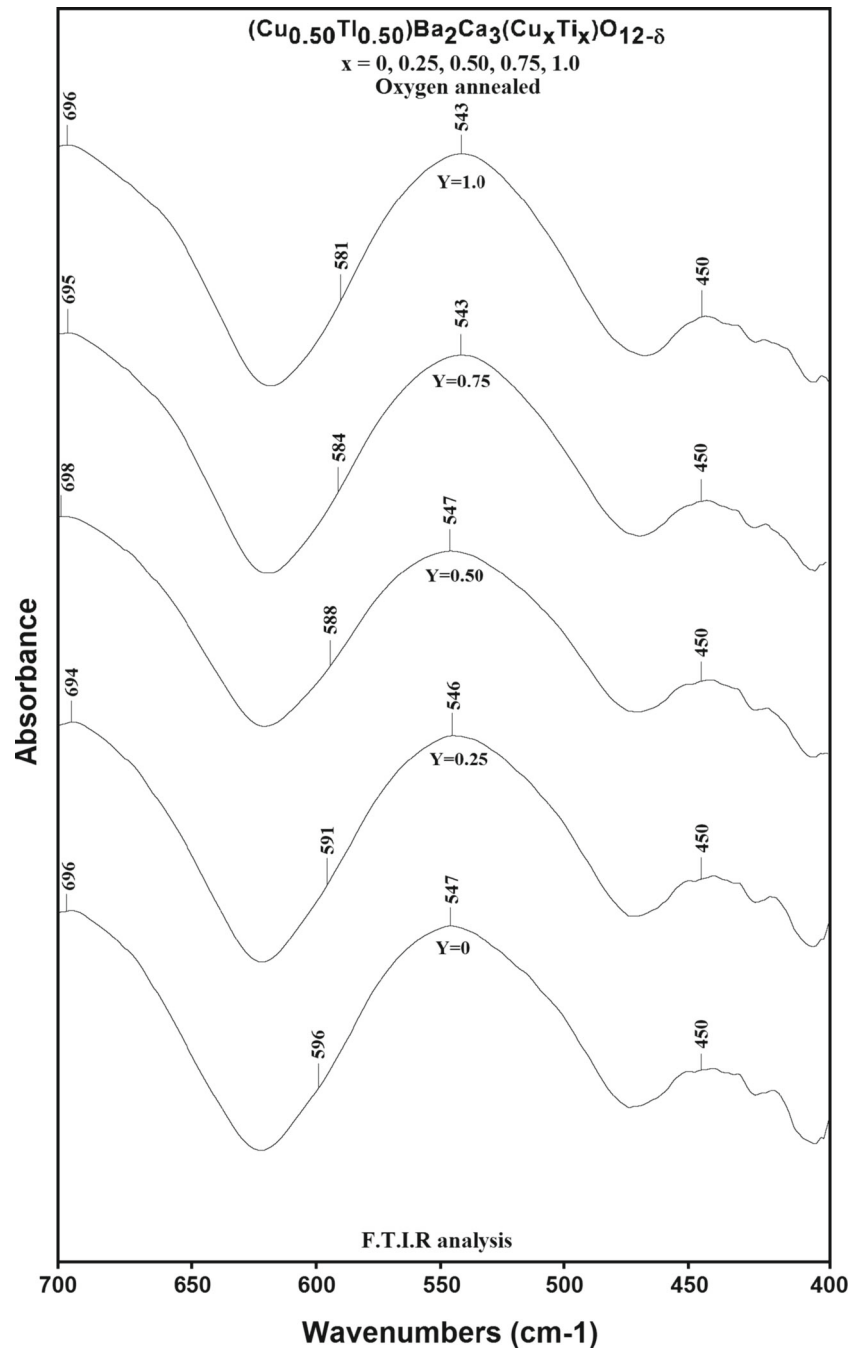
$$T_0 = T_c \left[1 + \left(\frac{2\xi_c(0)}{d} \right)^2 \right]$$

The second term is the interlayer coupling strength, which is related to the reduced temperature ε by $J = \varepsilon / 4$. In

layered superconductors at very low temperature close to zero resistivity temperature $\xi_c > d$, where d is the distance between the superconducting layers of adjacent unit cells (d is approximately equal to the c -axis lattice parameter of the unit cell). The advantage of LD model is that it reduces to 2D AL model for large ε values where the coupling constant J is quite small and to 3D AL model for small ε values where in some cases the coupling constant J is quite strong. The above theoretical AL and LD models are based on direct contribution to the excess conductivity.

There is one more region of fluctuations close to critical temperature for which $\lambda = 1/3$ and is known as critical region [21]. Some authors have observed a cross-over to 0D fluctuations with critical exponent 2. In high T_c superconductors, the MT contribution, which is due to the interaction of fluctuating Cooper pairs with normal electrons, is not easily observable. Since the MT contribution is negligible in cuprate superconductors [22]. This indirect contribution to the excess conductivity was calculated by Maki [23] and later on modified by Thompson [24]. For layered

Fig. 6 FTIR measurements of oxygen-annealed $(\text{Cu}_{0.5}\text{Tl}_{0.5})\text{Ba}_2\text{Ca}_3(\text{Cu}_x\text{Ti}_y)\text{O}_{12-\delta}$ $\text{Ba}_2\text{Ca}_3(\text{Cu}_{4-y}\text{Ti}_y)\text{O}_{12-\delta}$ ($y = 0, 0.25, 0.50, 0.75, 1.0$) samples



superconductors, Hikami and Larkin [25] derived the indirect contribution to the excess conductivity independently by Maki and Thompson [26, 27]:

$$\Delta\sigma_{\text{MT}} = \left[\frac{e^2}{8\hbar d\varepsilon \left(1 - \frac{\alpha}{\delta}\right)} \right] \ln \left[\left(\frac{\alpha}{\delta} \right) \left(\frac{1 + \alpha + (1 + 2\alpha)^{1/2}}{1 + \delta + (1 + 2\delta)^{1/2}} \right) \right]$$

where δ

$$\delta = \left[\left(\frac{4\xi_c(0)}{d} \right)^2 \left(\frac{k_B T \tau_\phi}{\pi \hbar} \right) \right]$$

is the pair-breaking parameter, which was introduced by Thompson [24] and is related to in-elastic scattering processes that limit the phase relaxation time τ_ϕ of the

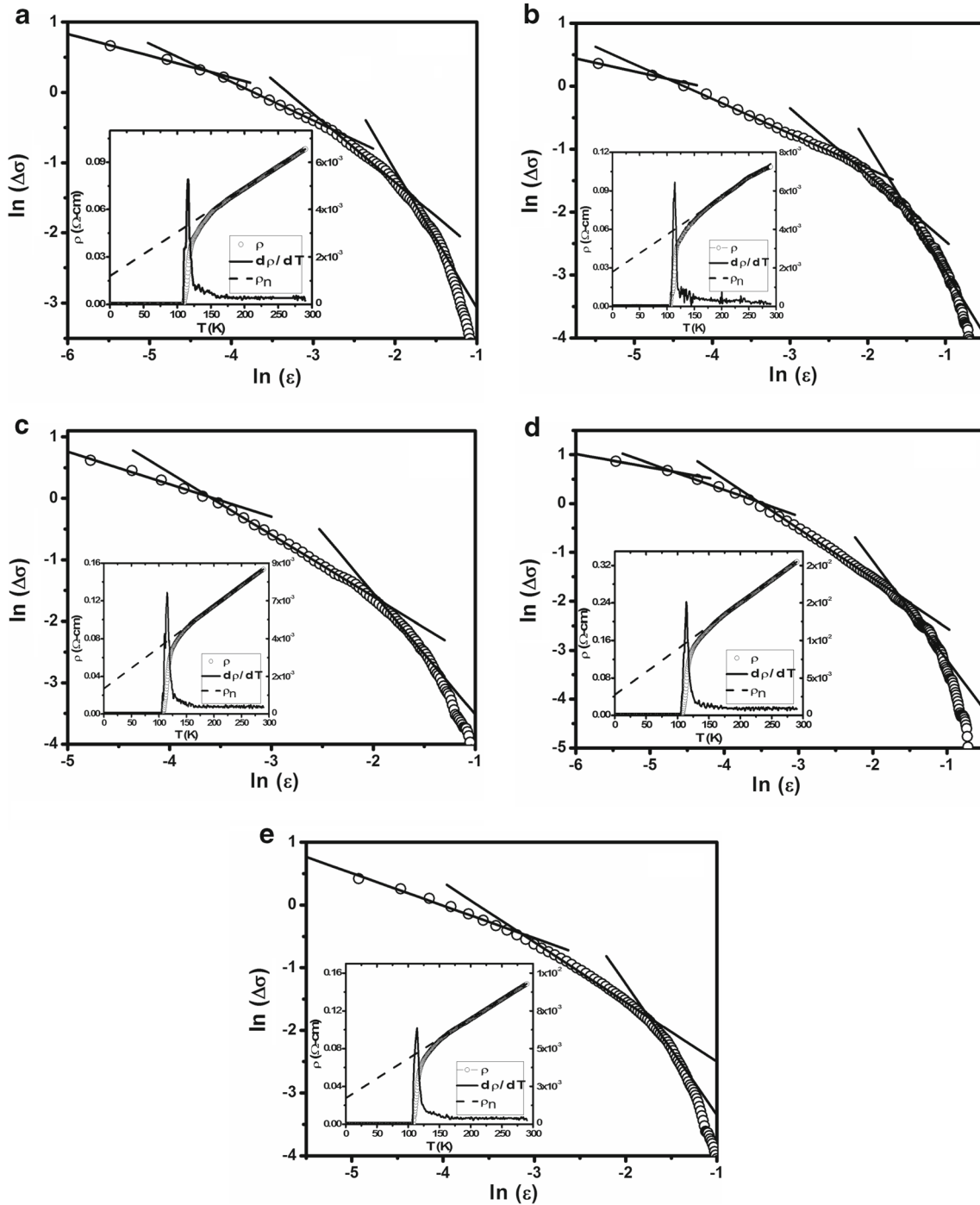


Fig. 7 (a, b, c, d, e): $\ln(\Delta\sigma)$ versus $\ln(\varepsilon)$ plots of $(\text{Cu}_{0.5}\text{Tl}_{0.5})\text{Ba}_2\text{Ca}_3(\text{Cu}_{4-y}\text{Ti}_y)\text{O}_{12-\delta}$ ($x=0, 0.25, 0.50, 0.75, 1.0$) superconductors; (a) $x=0$, (b) $x=0.25$, (c) $x=0.50$, (d) $x=0.75$, (e) $x=1.0$ (In the insets are shown the experimentally measured dc-resistivity ρ ($\Omega\text{-cm}$),

derivative ($d\rho/dT$) of dc-resistivity versus temperature, and the straight line extrapolated from the room temperature “300 K” normal state resistivity to 0 K)

quasiparticles involved in MT process [28] and k_B is the Boltzmann constant. In s-wave BCS superconductor, nonmagnetic impurities neither change T_c nor affect AL and MT terms, while on the other hand, in p- or d-wave superconductor, these impurities may act pair-breaking and are supposed to suppress the MT contribution [28].

The cross-over from 2D AL to 0D MT fluctuation contribution occurs at a temperature where $\delta \approx \alpha$, which gives [29]

$$\varepsilon_o \approx \left[\frac{\pi \hbar}{1.203 \left(\frac{l}{\xi_{ab}} \right) (8k_B T \tau_\varphi)} \right]$$

When the mean free path l of the Cooper pairs approaches to ξ_{ab} at a particular temperature then the Cooper pairs are broken to Fermions and at that temperature the phase relaxation time can be estimated as

$$\tau_\varphi = \left[\frac{\pi \hbar}{8k_B T \varepsilon_0} \right]$$

Fermi velocity of the carriers can also be estimated by

$$V_F \approx \left[\frac{5\pi k_B T_c \xi_c(0)}{2K \hbar} \right]$$

where $K \approx 0.12$ is a co-efficient of proportionality [30]. Fermi energy of the carriers can also be calculated by

$$E_F \approx \frac{1}{2} m^* V_F^2$$

where $m^* = 10m_o$ is the effective mass of the carrier and m_o is the carrier free mass [31].

Ginzburg and Landau observed the existence of two types of superconductors depending upon the energy of the interface between the normal and superconducting states. In 1957, Alexei Abrikosov used Ginzburg–Landau theory to explain the experimental data of superconducting alloys and thin films. He found that high magnetic field in a type II superconductor penetrates in the form of magnetic flux quanta Φ_o . The thermodynamics magnetic field $B_c(0)$ can be estimated from Ginzburg number N_G , which is given by [31, 32]

$$N_G = \left| \frac{T_G - T_c^{mf}}{T_c^{mf}} \right| = \frac{1}{2} \left(\frac{k_B T_c \gamma}{\{B_c(0)\}^2 \{\xi_c(0)\}^3} \right)^2$$

where $\gamma = \xi_{ab}(0)/\xi_c(0)$ is anisotropy, and T_G is the cross-over temperature from critical to 3D regime. We can estimate penetration depth $\lambda_{p,d}$, lower critical magnetic field $B_{c1}(0)$, upper critical magnetic field $B_{c2}(0)$, and the critical

current density $J_{c(0)}$ after determination of $B_c(0)$ as follows [33–36]:

$$B_c = \frac{\Phi_o}{2\sqrt{2}\lambda_{p,d}\xi_{ab}(0)}$$

$$B_{c1} = \frac{B_c}{\kappa\sqrt{2}} \ln \kappa$$

$$B_{c2} = \sqrt{2}\kappa B_c$$

$$J_c = \frac{4\kappa B_{c1}}{3\sqrt{3}\lambda_{p,d} \ln \kappa}$$

where $\Phi_o = \hbar/2e$ is the flux quantum, and κ is the GL parameter, which is the ratio of penetration depth to coherence length.

4 Results and Discussion

The x-ray diffraction scans of $(\text{Cu}_{0.5}\text{Tl}_{0.5})\text{Ba}_2\text{Ca}_3(\text{Cu}_{4-y}\text{Ti}_y)\text{O}_{12-\delta}$ ($y = 0, 0.25, 0.50, 0.75, 1.0$) as-prepared samples are shown in Fig. 1a–e. The planar reflections are best fitted to the tetragonal crystal structure following P4/MMM space group. The c -axis length suppresses, whereas the a -axis length increases with Ti doping (Fig. 2). The resistivity versus temperature measurements of oxygen-post-annealed $(\text{Cu}_{0.5}\text{Tl}_{0.5})\text{Ba}_2\text{Ca}_3(\text{Cu}_{4-y}\text{Ti}_y)\text{O}_{12-\delta}$ ($y = 0, 0.25, 0.50, 0.75, 1.0$) samples is shown in Fig. 3. Metallic variation of resistivity from room temperature down to an onset temperature of superconductivity is a typical feature of these samples. The as-prepared samples have shown the onset of superconductivity around 124.6, 118.7, 117.7, 116.1, and 120 K and the zero resistivity critical temperature $T_c(R = 0)$ at 108.4, 100.1, 97, 94.4, and 99 K, respectively, while the oxygen-annealed samples have shown the onset of superconductivity around 124.5, 122, 122, 121, and 120 K and the zero resistivity critical temperature of 110, 109, 109, 107, and 106 K, respectively. The enhancement in $T_c(\text{onset})$ and $T_c(R = 0)$ with oxygen post-annealing arises most likely due to suppression in the population of inadvertent oxygen defects due to oxygen doping in the unit cell (Fig. 4). Oxygen doping optimizes the density of the carriers in the conducting $\text{CuO}_2/\text{TiO}_2$ planes that in turn enhance the $T_c(\text{onset})$, $T_c(R = 0)$, and the magnitude of superconductivity. The AC susceptibility measurements of oxygen-post-annealed $(\text{Cu}_{0.5}\text{Tl}_{0.5})\text{Ba}_2\text{Ca}_3(\text{Cu}_{4-y}\text{Ti}_y)\text{O}_{12-\delta}$ ($y = 0, 0.25, 0.50, 0.75, 1.0$) samples are displayed in Fig. 5. The onset of diamagnetism is observed in these samples around 104, 119, 111, 118, and 103 K, respectively. Except in the samples with Ti doping of $y = 1$, all the samples have shown increases in the magnitude of diamagnetism and it seems to be the solubility limit of Ti doping in $(\text{Cu}_{0.5}\text{Tl}_{0.5})\text{Ba}_2\text{Ca}_3(\text{Cu}_{4-y}\text{Ti}_y)\text{O}_{12-\delta}$ samples. The FTIR absorption measurements of $(\text{Cu}_{0.5}\text{Tl}_{0.5})\text{Ba}_2\text{Ca}_3$

Table 1 Parameters estimated from $\ln(\Delta\sigma)$ and $\ln(\varepsilon)$ plots

Sample	λ_{CR}	λ_{3D}	λ_{2D}	λ_{SW}	$T_{CR-3D} = T_G$ (K)	T_{3D-2D} (K)	T_{2D-SW} (K)	T_{cmf} (K)	T^* (K)	$\alpha = \rho_n(0\text{ K})$ ($\Omega\text{-cm}$)	$W = \Delta T_c$ (K)
Ti “0”	0.31	0.54	0.98	1.97	117.7	122.5	135.1	116.0	147.2	0.018	5.49
Ti “0.25”	0.27	0.55	1.05	2.01	115.3	119.5	134.5	114.2	145.3	0.027	5.42
Ti “0.5”	–	0.53	1.00	1.97	115.8	117.7	130.8	115.1	144.8	0.027	7.53
Ti “0.75”	0.27	0.53	1.01	2.02	114.8	116.6	135.1	114.2	154.9	0.044	6.11
Ti “1.0”	–	0.52	0.96	2.09	115.3	118.8	135.6	115.1	142.4	0.028	6.52

$(\text{Cu}_{4-y}\text{Ti}_y)\text{O}_{12-\delta}$ ($y = 0, 0.25, 0.50, 0.75, 1.0$) oxygen-post-annealed samples are displayed in Fig. 6. The apical oxygen mode around 548 cm^{-1} is softened and observed around $547, 546, 547, 543,$ and 543 cm^{-1} for Ti doping of $y = 0, 0.25, 0.50, 0.75, 1.0,$ respectively. The peak position of the other apical oxygen mode around 450 cm^{-1} stays unchanged with the doping of Ti in final compound. Planar oxygen mode in oxygen-post-annealed samples is observed around $596, 591, 588, 584,$ and 581 cm^{-1} in $(\text{Cu}_{0.5}\text{Tl}_{0.5})\text{Ba}_2\text{Ca}_3(\text{Cu}_{4-y}\text{Ti}_y)\text{O}_{12-\delta}$ ($y = 0, 0.25, 0.50, 0.75, 1.0$) samples. The softening of apical oxygen modes along with planar oxygen is most likely due to doping of Ti in the unit cell, which changes the bond distances and hence their dipole moment thereby inducing the relaxation of bond distances.

The FIC analysis of the dc resistivity versus temperature data of $(\text{Cu}_{0.5}\text{Tl}_{0.5})\text{Ba}_2\text{Ca}_3(\text{Cu}_{4-y}\text{Ti}_y)\text{O}_{12-\delta}$ ($y = 0, 0.25, 0.50, 0.75, 1.0$) samples has been carried out by using the abovementioned models in the neighborhood of transition region. The plots of $\ln(\Delta\sigma)$ versus $\ln(\varepsilon)$ of $(\text{Cu}_{0.5}\text{Tl}_{0.5})\text{Ba}_2\text{Ca}_3(\text{Cu}_{4-y}\text{Ti}_y)\text{O}_{12-\delta}$ ($y = 0, 0.25, 0.50, 0.75, 1.0$) samples are shown in Fig. 7a–e. The experimentally measured dc resistivity $\rho(\Omega\text{-cm}^{-1})$ along with a straight line extrapolated from the room temperature (300 K) normal-state resistivity to 0 K and derivative ($d\rho/dT$) of dc resistivity versus temperature are shown in the

insets of Fig. 7a–e. The superconducting fluctuations start at a particular temperature denoted by T^* from where the experimental dc resistivity curve deviates from the straight line extrapolated from the room temperature normal-state resistivity to zero K. The values of T^* are around 147.2, 145.3, 144.8, 154.9, and 142.4 K for $y = 0, 0.25, 0.50, 0.75,$ and $1.0,$ respectively. The decrease in values of T^* show that the superconducting fluctuations shift to the lower temperature values, which is most likely due to increased doping concentration of Ti (47.90 amu) atoms which has smaller mass in comparison with Cu (63.54 amu) atoms that induce an-harmonic oscillation in the $\text{CuO}_2/\text{TiO}_2$ planes, thereby suppressing the density of phonons. If electron–phonon interaction was essential for the mechanism of high T_c superconductivity, the decrease in the density of phonon modes would suppress the population of the Cooper pairs and the essential superconductivity parameters depending on their density. The values of critical exponents ($\lambda_{CR}, \lambda_{3D}, \lambda_{2D},$ and λ_{0D}), cross-over temperatures ($T_{CR-3D} = T_G, T_{3D-2D},$ and T_{2D-SW}), mean field critical temperature (T_{cmf}), T^* , residual resistivity (α), and superconducting transition width ($W = \Delta T_c$) deduced from the FIC analyses of $(\text{Cu}_{0.5}\text{Tl}_{0.5})\text{Ba}_2\text{Ca}_3(\text{Cu}_{4-y}\text{Ti}_y)\text{O}_{12-\delta}$ ($y = 0, 0.25, 0.50, 0.75, 1.0$) samples are given in Table 1. All the cross-over temperatures, T_{cmf} , and T^* have been shifted to the lower temperature values. The various superconductivity

Table 2 Superconducting parameters estimated from excess conductivity

Sample	$\xi_c(0)$ (\AA)	J	N_G	$\lambda_{p,d}$ (\AA)	$B_c(0)$ (T)	B_{c1} (T)	B_{c2} (T)	κ	$J_c(0) * 10^3$ (A/cm^2)	$V_F * 10^7$ (m/s)	E_{Break} (eV)	$\tau_\varphi * 10^{-14}$
Ti “0”	2.13	0.056	0.066	890.1	1.63	0.083	128.7	55.6	0.99	2.01	0.04	9.94
Ti “0.25”	1.94	0.046	0.053	737.5	1.97	0.116	128.7	46.1	1.45	1.81	0.04	9.76
Ti “0.5”	1.35	0.023	0.066	452.5	3.21	0.268	128.7	28.2	3.86	1.25	0.04	11.2
Ti “0.75”	1.34	0.022	0.073	467.8	3.11	0.254	128.7	29.2	3.62	1.23	0.05	8.44
Ti “1.0”	1.58	0.030	0.087	623.2	2.33	0.155	128.7	38.9	2.03	1.43	0.05	7.96

parameters (i.e., $\xi_c(0)$, J , N_G , $\lambda_{p,d}$, $B_c(0)$, B_{c1} , B_{c2} , κ , J_c , V_F , E_{Break} , and τ_φ) deduced from the FIC analysis of $(\text{Cu}_{0.5}\text{Ti}_{0.5})\text{Ba}_2\text{Ca}_3(\text{Cu}_{4-y}\text{Ti}_y)\text{O}_{12-\delta}$ ($y = 0, 0.25, 0.50, 0.75, 1.0$) samples are given in Table 2. The values of $\xi_c(0)$, J , N_G (except $y = 0.75$ and 1.0), $\lambda_{p,d}$, κ , V_F , and τ_φ (except $y = 0.50$) have been decreased by Ti doping in the final compound showing the electron–phonon interaction different from BCS is essential for mechanism of high T_c superconductivity in oxides. The values of parameters such as B_c , B_{c1} , $J_{c(0)}$ got increased with increase in Ti content. It is most likely that population agglomerate of Ti/Cu/Ba/Ca/O_y at the grain boundaries with the increase Ti doping which act as efficient pinning centers which result in increase in the values of B_c , B_{c1} , and $J_{c(0)}$.

5 Conclusions

$(\text{Cu}_{0.5}\text{Ti}_{0.5})\text{Ba}_2\text{Ca}_3(\text{Cu}_{4-y}\text{Ti}_y)\text{O}_{12-\delta}$ ($y = 0, 0.25, 0.50, 0.75, 1.0$) superconductors are prepared by two-step solid state reaction method at 880 °C. In order to optimize the density of carriers in the CuO_2 planes, the samples were annealed in the flowing oxygen environment at 500 °C for approximately 5 h. These samples have shown tetragonal crystal structure with a -axis length increasing, whereas the c -axis decreasing with increased Ti doping. The samples are characterized by resistivity, ac susceptibility, and FTIR absorption measurements. The magnitude of superconductivity also suppresses with increase in Ti doping. In FTIR absorption measurements, oxygen-annealed $(\text{Cu}_{0.5}\text{Ti}_{0.5})\text{Ba}_2\text{Ca}_3(\text{Cu}_{4-y}\text{Ti}_y)\text{O}_{12-\delta}$ ($y = 0, 0.25, 0.50, 0.75, 1.0$) samples have shown that the peak position of the apical oxygen mode around 450 cm^{-1} stays unchanged, while the peak positions for the apical oxygen mode around 548 cm^{-1} along with the planar oxygen modes are softened with the doping of Ti in final compound. We proposed this to be arising due to the doping of Ti (47.90 amu) atoms at Cu (63.54 amu) sites that results in the decrease values of superconductivity parameters. A possible correlation of suppression of superconductivity parameters is attributed to the presences of atoms of different masses in $\text{CuO}_2/\text{TiO}_2$ planes which induce an-harmonic oscillations, thereby suppressing the phonon population. The phonons of harmonic oscillation with wave vector q and the an-harmonic oscillation with wave vector q' produce a new phonon with wave vector Q that do not contribute in the Cooper pair formation. It suppresses the density of essential phonon required for the Cooper pair formation and hence the superconductivity. These studies show the essential role of electron–phonons

interactions in the mechanism of high T_c superconductivity. The results of excess conductivity analyses (FIC) support this conclusion. Along with the suppression of all cross-over temperatures, T_{cmf} , and T^* , a decrease in the values of $\xi_c(0)$, J , $\lambda_{p,d}$, κ , and V_F is observed. The increase in the values of B_c , B_{c1} , $J_{c(0)}$ most likely arises from the increase population of the pinning centers of agglomerates of Ti at the grain boundaries.

References

- Ihara, H., Sekita, Y., Tateai, H., Khan, N.A., Ishida, K., Harashima, E., Kojima, T., Yamamoto, H., Tanaka, K., Tanaka, Y., Terada, N., Obara, H.: IEEE Trans. Appl. Supercond. **9**, 1551 (1999)
- Khan, N.A., Khuram, A.A., Maqsood, A.: Physica C **398**, 114 (2003)
- Tokunaga, Y., Ishida, K., Kitaoka, Y., Asayama, K., Tokiwa, K., Iyo, A., Ihara, H.: Phys. Rev. B **61**, 9707 (2000)
- Hamdan, N.M.: Physica B **284**, 1093 (2000)
- Mikus, S., Urita, N., Hashinaka, Y., Tokiwa, K., Iyo, A., Tanaka, Y., Watanabe, T.: Physica C **442**, 91 (2006)
- Juang, J.Y., Horng, J.H., Chen, S.P., Fu, C.M., Wu, K.H., Uen, T.M., Gou, Y.S.: Appl. Phys. Lett. **66**, 885 (1995)
- Cheng, Z.X., Wang, X.L., Keshavarzi, S., Qin, M.J., Silver, T.M., Liu, H.K., Kimura, H., Dou, S.X.: Supercond. Sci. Technol. **17**, 696 (2004)
- Lu, R.T., Yan, S.L., Fang, L., He, M.: Supercond. Sci. Technol. **14**, 948 (2001)
- Schneidewind, H., Stelzner, T.: IEEE Trans. Appl. Supercond. **13**, 2762 (2003)
- Duhalde, S., Lamagna, A., Villafuerte, M., Schwartzman, A., Corra, L., Quintana, G.: Appl. Surf. Sci. **127**, 520 (1998)
- Mumtaz, M., Khan, N.A., Khan, E.U.: Physica C **470**, 428–434 (2010)
- Mumtaz, M., Khan, N.A., Ashraf, F.: J. Supercond. Nov. Magn. **24**, 1985–1989 (2011)
- Mumtaz, M., Khan, N.A., Nawaz, R.: J. Supercond. Nov. Magn. **23**, 565–569 (2010)
- Khan, N.A., Rahim, M.: J. Alloys Compd. **481**, 81 (2009)
- Rahim, M., Khan, N., Awazish, A.: J. Alloys Compd. **513**, 55 (2011)
- Aslamazov, L.G., Larkin, A.L.: Phys. Lett. A **26**, 238 (1968)
- Lawrence, W.E., Doniach, S.: In: Kanda, E. (ed.) Proceedings of the Twelfth International Conference on Low Temperature Physics, p. 361. Keigaku (1971)
- Solovjov, A.L., Habermeier, H.-U., Haage, T.: Low Temp. Phys. **28**, 17–24 (2002)
- Passos, C.A.C., Orlando, M.T.D., Passamai Jr., J.L., de Mello, E.V.L., Correa, H.P.S., Martinez, L.G.: Phys. Rev. B **74**, 094514 (2006)
- Ghorbani, S.R., Rahmati Tarki, M.: J. Supercond. Novel Magn. **27**, 749 (2014)
- Han, S.H., Eltsev, Yu., Rapp, Ö.: Phys. Rev. B **61**, 11776 (2000)
- Naqib, S.H., Cooper, J.R., Tallon, J.L., Islam, R.S., Chakalov, R.A.: Phys. Rev. B **71**, 054502 (2005)
- Maki, K.: Prog. Theor. Phys. **39**, 897 (1968)
- Thompson, R.S.: Phys. Rev. B **1**, 327 (1970)
- Hikami, S., Larkin, A.I.: Mod. Phys. Lett. B **2**, 693 (1988)

26. Maki, K., Thompson, R.S.: *Phys. Rev. B* **39**, 2767 (1989)
27. Nayak, P.K., Ravi, S.: *Supercond. Sci. Technol.* **19**, 1209 (2006)
28. Lang, W., Heine, G., Kula, W., Sobolewski, R.: *Phys. Rev. B* **51**, 9180 (1995)
29. Solovjov, A.L., Habermeier, H.-U., Haage, T., Nizk, F.: *Low Temp. Phys.* **28**, 99 (2002)
30. Bardeen, J., Cooper, L.N., Schrieffer, J.R.: *Phys. Rev.* **108**, 1175 (1957)
31. Solovjov, A.L., Dmitriev, V.M., Habermeier, H.-U.: *Phys. Rev. B* **55**, 8551 (1997)
32. Ihara, H., Iyo, A., Tanaka, K., Tokiwa, K., Ishida, K., Terada, N., Tokumoto, M., Sekita, Y., Tsukamoto, T., Watanabe, T., Umeda, M.: *Physica C* **1973**, 282–287 (1997)
33. Abou Aly, A.I., Ibrahim, I.H., Awad, R., El-Harizy, A., Khalaf, A.: *J. Supercond. Novel Magn.* **23**(7), 1325–1332 (2010)
34. Annet, J.F.: *Superconductivity, Superfluids and Condensates*. Oxford University Press, London (2004)
35. Khan, N.A., Ahmad, S.: *J. Appl. Phys.* **112**, 033912 (2012)
36. Mohammad, N.H., Abou-Aly, A.I., Awad, R., Ibrahim, I.H., Roumie, M., Rekaby, M.: *J. Low Temp. Phys.* **172**, 234–255 (2013)